Science Signaling
AAAS
www.sciencesignaling.org/cgi/content/full/4/157/ra4/DC1

Supplementary Materials for

Genome-Wide RNAi Screen Reveals Disease-Associated Genes That Are Common to Hedgehog and Wnt Signaling

Leni S. Jacob, Xiaofeng Wu, Michael E. Dodge, Chih-Wei Fan, Ozlem Kulak, Baozhi Chen, Wei Tang, Baolin Wang, James F. Amatruda, Lawrence Lum*

*To whom correspondence should be addressed. E-mail: lawrence.lum@UTSouthwestern.edu

Published 25 January 2011, *Sci. Signal.* **4**, ra4 (2011)
DOI: 10.1126/scisignal.2001225

This PDF file includes:

Other Supplementary Material for this manuscript includes the following:
(available at www.sciencesignaling.org/cgi/content/full/4/157/ra4/DC1)

Figure S1

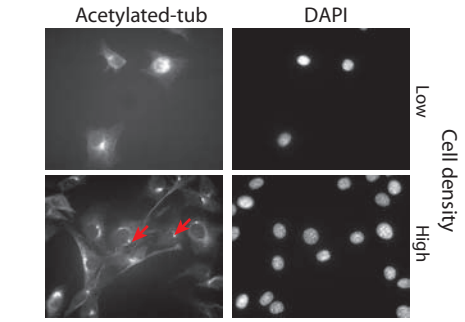

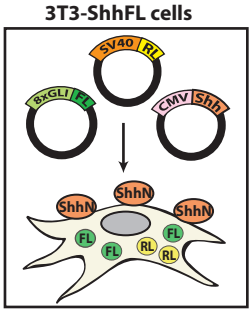

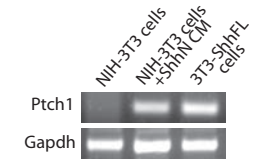

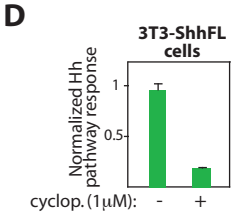

E

Assay	Conditions	Cutoffs
Primary Screen	NIH3T3-ShhFL; 72 hrs	Z (FL) ≤ -2.0; SD < 0.10; |Z (RL)| < 2.5
Exogenous Hh Test	Light II cells; 72 hrs	FL ≤ 75% control; SD < 0.15
Wnt Assay	NIH-3T3 cells; 72hrs	90%≤ FL/RL ≤110%
Cross-Library Test	Light II cells; 72 hrs	FL ≤ 75% control; SD < 0.15

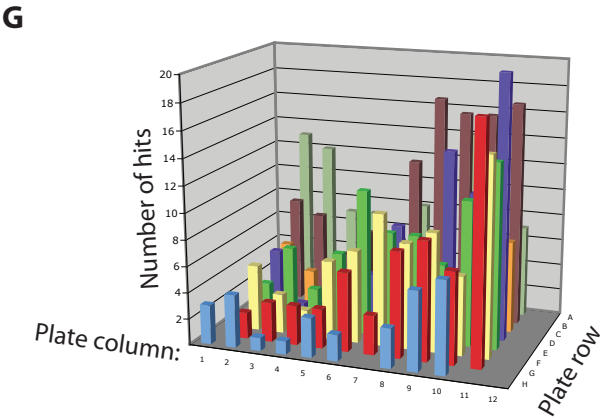

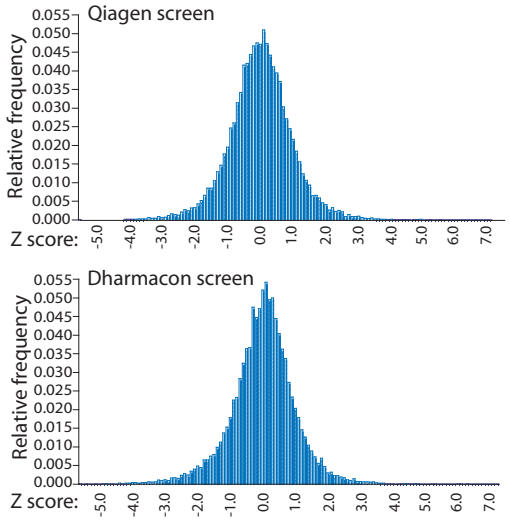

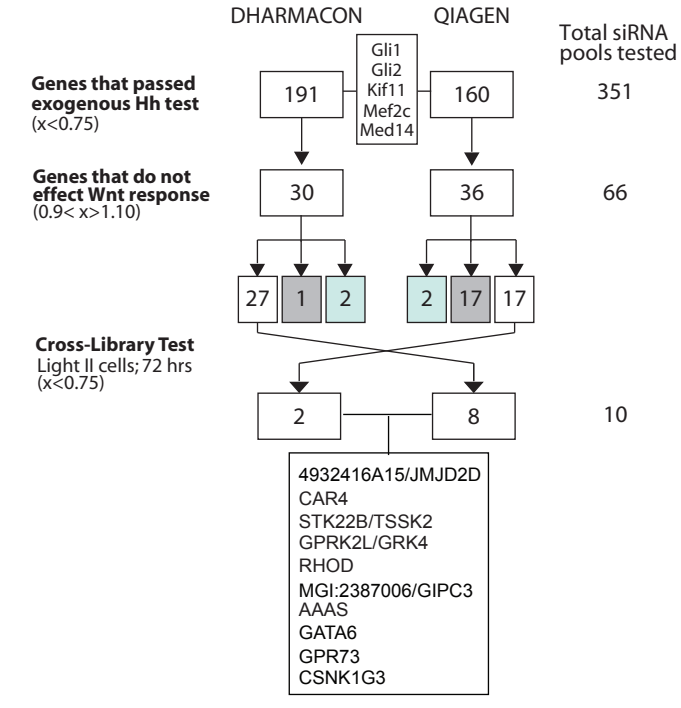

Figure S1. Additional material relating to the RNAi screen. A. NIH-3T3 cells form cilia under high-density conditions. **B.** A cell-autonomous signaling assay for Hh pathway response. NIH-3T3 cells were stably integrated with an Hh-responsive firefly luciferase (FL) reporter (GliBS reporter), a control reporter (Renilla luciferase; RL), and an expression construct encoding Shh to generate the 3T3-ShhFL cell line. **C.** 3T3-ShhFL cells exhibit faithful Hh transcriptional response. RT-PCR analysis of the Hh target gene Ptch1 in 3T3-ShhFL cells was compared with wild-type NIH-3T3 cells treated with or without ShhN conditioned medium. **D.** 3T3-ShhFL cells are responsive to cyclopamine. **E.** Criteria and conditions used to select genes of interest in the primary screen and various secondary screens. **F.** Frequency of Z score assignment to genes reveals a Gaussian-type distribution of results. **G.** Summary of hits identified from various well positions in 96 well plates from the primary screen without well-based normalization procedure. An edge effect is apparent from the skewed well distribution of hit frequenices. **H.** Genes identified from screening either the Dharmacon or Qiagen libraries that do not effect Wnt pathway response (62 total) were re-tested manually in 96 well plates avoiding wells on the edge of the plate using siRNAs targeting the same gene from the other library. A total of 18 genes could not be re-tested given a corresponding siRNA set was not arrayed in the library. Ten genes including several identified from the OMIM-based analysis were shown to induce similar effects on Hh pathway response. The improved ability to recover shared genes from both siRNA libraries but not necessary known pathway components (Smo for example) under these testing conditions demonstrate the influence of siRNA design and inherent noise in high-throughput screening platforms in genome-scale RNAi studies. White boxes- genes that were tested; gray boxes - genes not tested because there is no corresponding gene in the other library; blue boxes- genes that have already been identified by 2 pools, thus not tested in the cross-library test.

Figure S2

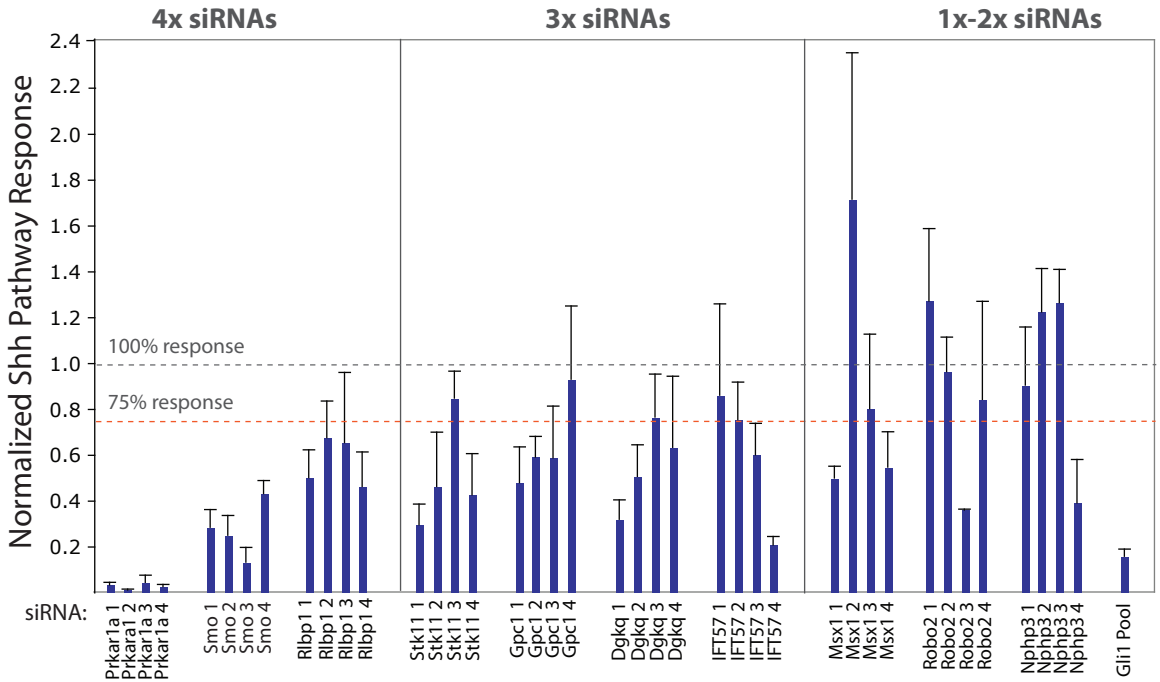

Figure S2. Confirmatory siRNA assays for gene function in Hh pathway response. Disease-associated genes identified in Fig. 1 were re-evaluated using non-redundant siRNAs from each siRNA pool. Gene function in Hh pathway response confirmed by only one or two siRNAs was no longer considered. Data are represented as mean +/– SEM.

Figure S3

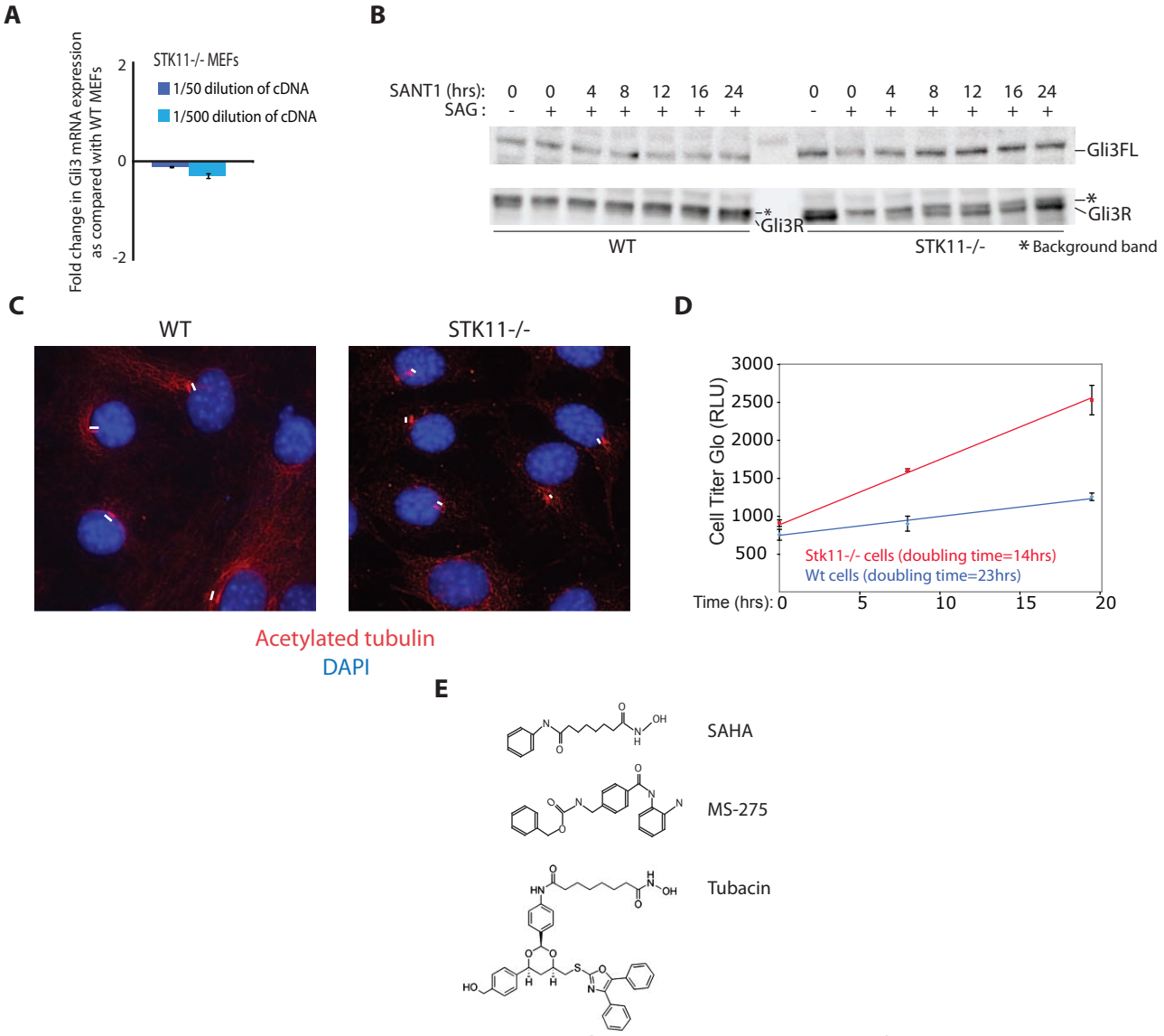

Figure S3. Additional characterization of *STK11*$^{-/-}$ cells. A. Wt and *STK11*$^{-/-}$ MEFs express comparable levels of Gli3. A. PCR was performed from different concentrations of total cDNA generated from RNA samples, analyzed, and compared to test reproducibility. Gli3 transcript abundance cells is normalized to GapDH. Values are given as the fold change between Stk11-/- cells and WT cells. Graph shows average and SD from 3 samples. **B.** Raw data for analysis of kinetics Gli3R formation following addition of SAG quantified in Fig. 2F. In this study wild-type and STK11-/- MEFs were treated overnight with SAG (Smo agonist) to inhibit Gli3R formation. SAG was then removed and SANT1 was added to allow Gli3R formation. Lysate generated at various time points after SAG removal were analyzed by Western blot analysis for Gli3R protein then quantified as before. **C.** Additional images of primary cilia from WT and STK11-/- MEFs. White bars indicate length of the primary cilium. **D.** STK11-/- MEFs exhibit increased rate of doubling time as compared to WT MEFs. Cell number was measured using Cell Titer Glo assay that determines levels of ATP produced by cells. This experiment was performed in triplicate. **E.** Chemical structures of several classes of HDAC inhibitors. Tubacin and MS-275 exhibit selectivity for HDAC6 and HDAC1, respectively.

Figure S4

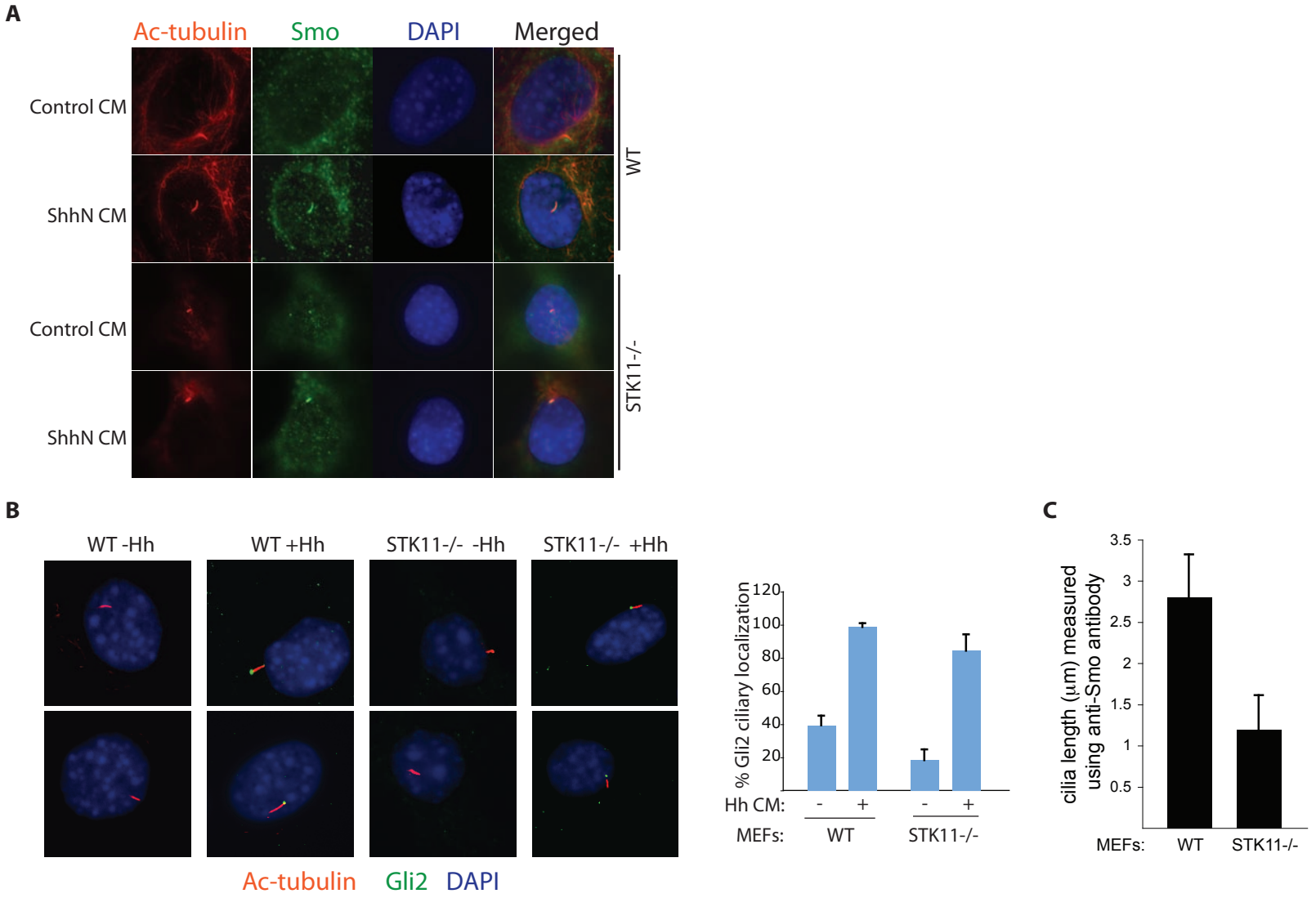

Figure S4. Hh-induced Smo or Gli protein accumulation in the primary cilium is not affected in *STK11*$^{-/-}$ cells. A. Endogenous Smo protein and acetylated tubulin were detected by immunofluorescence. **B.** Gli2 protein localizes to the tip of the primary cilium in STK11-/- MEFs treated with Hh conditioned medium. **C.** Quantification of cilia length in MEFs using an anti-Smo antibody.

Figure S5

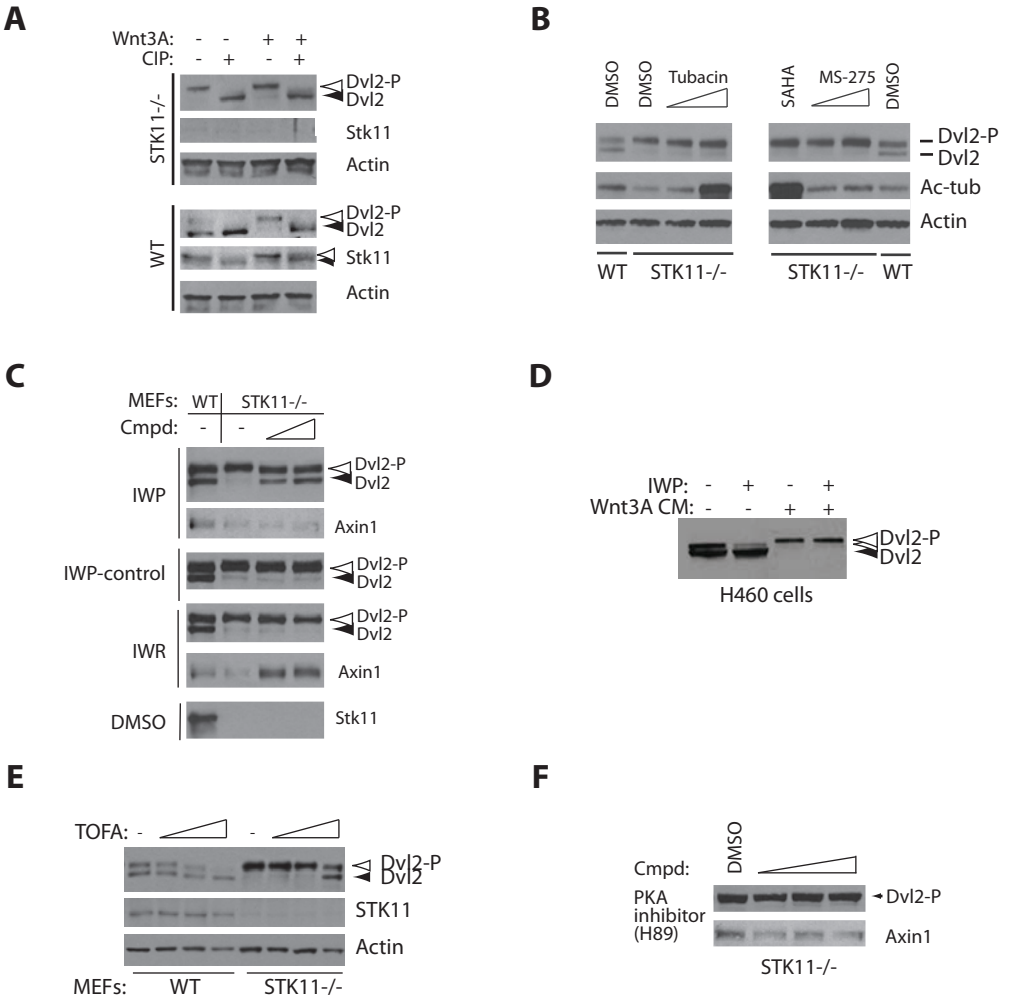

Figure S5. Dvl phosphorylation is sensitive to IWP but not SAHA. A. Dvl2 is phosphorylated in STK11-/- cells. Phosphatase treatment of cell lysates derived from STK11-/- cells confirms the slower migrating band recognized by the Dvl2 antibody as phosphorylated Dvl protein. CIP= calf intestinal phosphatase. **B.** Inhibition of HDAC6 does not alter Dvl protein phosphorylation. Tubacin and SAHA but not MS-275, an inhibitor HDAC1-3, induces accumulation of acetylated tubulin in agreement with their relative activity against HDAC6. **C.** The increased Dvl phosphorylation in STK11-/- cells is inhibited by IWP, but not IWR, an Axin protein stabilizer. In addition, an inactive form of IWP (IWP control) has no effect on Dvl phosphorylation. Abundance of Axin protein is used to monitor activity of IWR compound. Taken together, this data indicates that Dvl phosphorylation is dependent on production of Wnt. Data are representative of 3 experiments. **D.** The effects of IWP compound on Dvl2 phoshporylation can be blocked by addition of Wnt3A-containing conditioned medium (CM), consistent with the ability of IWP to inhibit Wnt protein production. **E.** The acetyl-coA (ACC) enzyme inhibitor TOFA mimics the effects of IWP on Dvl2 phosphorylation in wild-type and STK11-/- MEFs. Given the role of ACC in the production of palmitoyl-CoA, a co-factor essential to Wnt protein production, this observation further supports previous conclusions that the IWP compounds to inhibit Wnt protein production. F. Inhibition of PKA does not block Dvl2 phosphorylation in STK11-/- cells. STK11-/- MEFs were treated with increasing concentration of the PKA inhibitor H89 up to 10μM. Axin1 serves as a loading control.

Figure S6

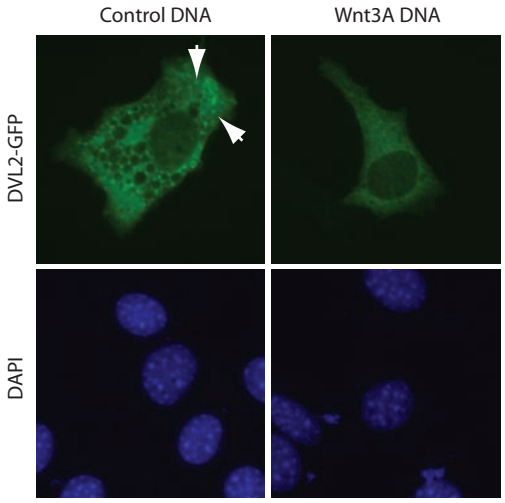

Figure S6. Dvl2 undergoes a change in distribution in response to Wnt protein stimulation in MEFs.
White arrows: Dvl2 punctae.

Figure S7

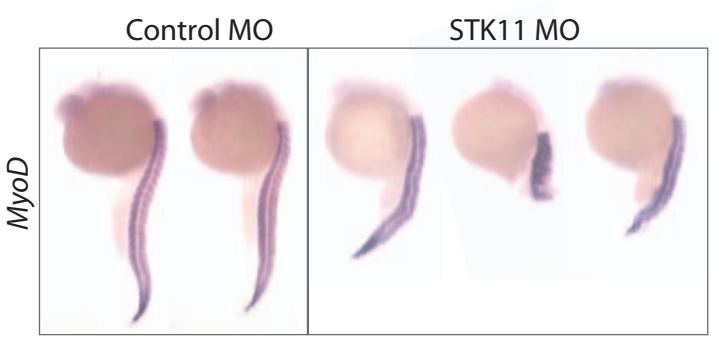

Figure S7. The defect in posterior morphogenesis and somite development is apparent in *STK11* morphants stained for *MyoD* expression, which labels somitic tissue. >25 embryos at 24 hrs post fertilization were analyzed in each group.

Figure S8

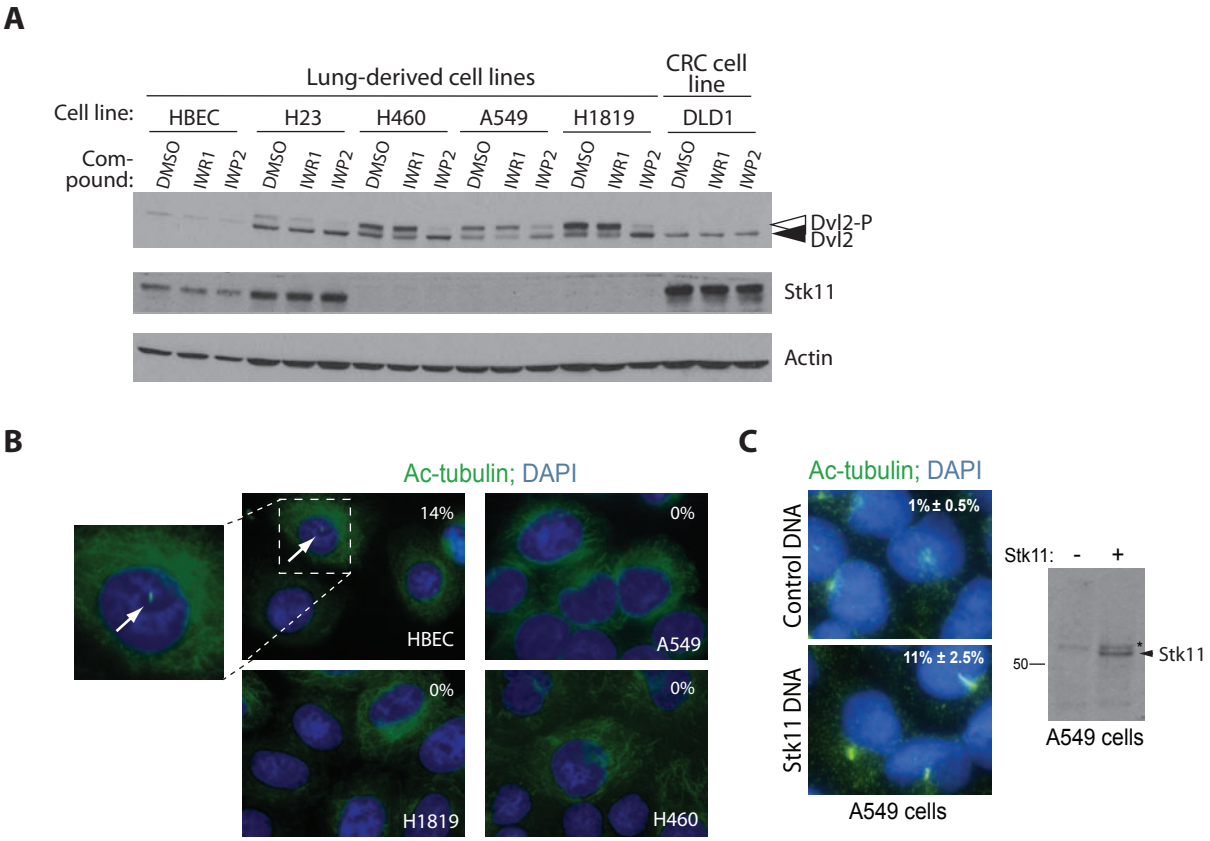

Figure S8. Loss of *STK11* in cancerous cells induces Dvl protein phosphorylation and compromises primary cilia formation. A. NSCLC cell lines lacking Stk11 exhibit increased abundance of phosphorylated Dvl protein that can be lowered with IWP compound. Human bronchial epithelial cells (HBEC) and colorectal cancer cells (DLD-1) are controls. **B.** NSCLC cell lines with loss of STK11 do not elaborate primary cilia as compared to HBECs. **C.** Introduction of Stk11 DNA into A549 cells increased the percentage of cells with primary cilium. Cells were selected for 7 days prior to immunostaining with an anti-acetylated tubulin antibody.

Figure S9

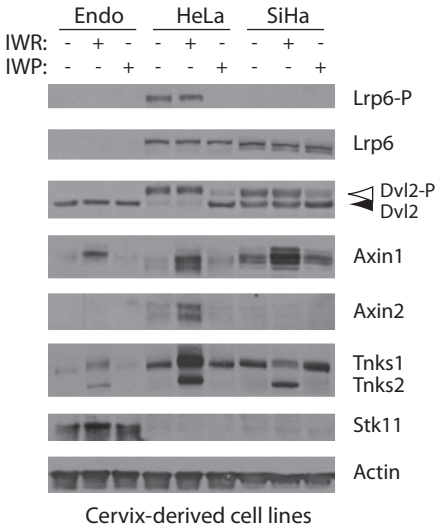

Figure S9. Cell line-dependent responses to Wnt ligand in cervical carcinoma cells lacking Stk11. Lysates from Endo, HeLa, or SiHa cells were Western blotted for various Wnt pathway components. As before, HeLa but not SiHa cells exhibit Wnt/β-catenin pathway response (measured by expression of Axin2) that is sensitive to the IWR and IWP compounds. In addition, HeLa cells exhibit phosphorylation of Lrp6, a receptor for mostly canonincal Wnt proteins. Dvl phosphorylation and Tankyrase (Tnks) protein levels are used to measure activity of IWP and IWR compounds, respectively. IWR compounds stabilize Axin proteins through the inhibition and stabilization of Tnks proteins, which facilitate Axin degradation.

Figure S10

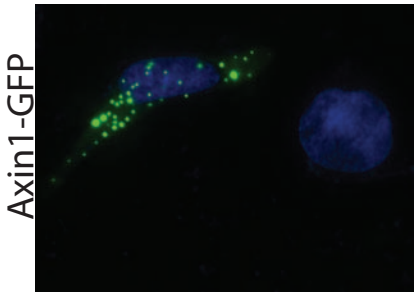

Figure S10. Axin1 forms punctate structures in HeLa cells. In contrast to the diffuse localization of Dvl2 in HeLa cells, its binding partner Axin1 is found in puncate structures.